

## Infrared Studies of the Onset of Conductivity in Ultrathin Pb Films

P. F. Henning,<sup>1,2</sup> C. C. Homes,<sup>1</sup> S. Maslov,<sup>1</sup> G. L. Carr,<sup>1</sup> D. N. Basov,<sup>2</sup> B. Nikolić,<sup>3</sup> and M. Strongin<sup>1</sup>

<sup>1</sup>Department of Physics, Brookhaven National Laboratory, Upton, New York 11973

<sup>2</sup>Department of Physics, University of California at San Diego, La Jolla, California 92093

<sup>3</sup>Department of Physics, SUNY at Stony Brook, Stony Brook, New York 11794

(Received 23 April 1999)

In this paper we report the first experimental measurement of the low-temperature, normal-state infrared conductivity of ultrathin quenched-condensed Pb films. For dc sheet resistances such that  $\omega\tau \ll 1$  the ac conductance increases with frequency but is in disagreement with the predictions of weak localization. We attribute this behavior to the effects of an inhomogeneous granular structure in these films when they are first formed, which is manifested at the very small probing scale of infrared measurements. Our data are consistent with predictions of two-dimensional percolation theory.

PACS numbers: 78.66.Bz, 74.76.Db, 72.15.Rn

Measurements of dc transport in ultrathin films have been a subject of active interest for many years [1]. These systems, consisting of a thin layer of metal deposited onto a substrate held at liquid helium temperatures, provide a relatively simple way to study the interplay between localization, electron-electron interactions, and superconductivity [2] in disordered quasi-2D metals. These experiments are in quantitative agreement with predictions of weak localization theory [3], combined with the effects of diffusion-enhanced electron-electron interactions [4]. The reason why this theory, developed for homogeneous materials, work so well in the case of granular, inhomogeneous films is that in dc transport experiments the relevant length scale is usually much larger than the characteristic size of inhomogeneities (grains themselves and the percolation clusters that form from them) in the film.

For the ac conductivity one can modify the characteristic transport length scale  $L_\omega = \sqrt{D/\omega}$  by simply changing the probing frequency (here  $D$  is the electron diffusion coefficient). In the frequency range, where  $L_\omega$  is smaller than all relevant dc length scales, one has a frequency-dependent weak localization correction to the conductivity [5]. This theory can account for a slow increase of the ac conductivity with frequency in the region  $\omega\tau \ll 1$ , where the Drude theory predicts a plateau. However, in our system these quantum effects constitute only one source of the frequency dependence of the conductivity. In the region where the material is strongly inhomogeneous the frequency dependence of conductivity is dominated by purely classical effects due to charge dynamics in a network of capacitively and resistively coupled clusters of grains. The effective way to describe these effects theoretically is provided by the framework of percolation theory [6]. In this theoretical approach the ac conductivity is shown to increase with frequency. Indeed, since the capacitive coupling between grains is proportional to the frequency, grains become more and more connected as the frequency is increased. While experimental data on the frequency dependence of the conductivity are virtually nonexistent for ultrathin quenched

condensed films, classical charge dynamics is known to play a dominant role in frequency dependence of the ac conductivity in thicker, more granular films, deposited onto a warm substrate [7]. It is also known that quantum corrections themselves become profoundly modified on length scales, where the material can no longer be treated as homogeneous [8].

In this Letter we report the first measurements of the conductivity of *ultrathin* films at infrared frequencies. Films used in these experiments were made *in situ* by evaporating Pb onto Si(111) (sets 1 and 2) and glass (set 3) substrates, mounted in an optical cryostat, held at 10 K. Ag tabs, predeposited onto the substrate, were used to monitor the dc resistance of the film. Infrared transmission measurements from 500 to 5000 cm<sup>-1</sup> (set 1), and 2500 to 8000 cm<sup>-1</sup> (sets 2 and 3) were made using a Bruker 113v spectrometer at the new high-brightness U12IR beam line at the BNL National Synchrotron Light Source. The substrates were covered with a 5 Å thick layer of Ge to promote two-dimensional thin-film growth, rather than the agglomeration of the deposited Pb in larger grains. For different depositions we observe a variation in the thickness where continuity first occurs. However, the optical properties of the films show rather similar behavior, as will be discussed below. We mention here that a remarkable feature of this behavior is a frequency-dependent conductivity that can be understood by classical arguments that assume an inhomogeneous structure on a nanoscale level. Films were evaporated at pressures ranging from the low 10<sup>-8</sup> to the mid 10<sup>-9</sup> Torr range. The transmission spectra were obtained after successive *in situ* Pb depositions. The dc resistances in set 1 on Si range from 64 MΩ/□ at 24.4 Å average thickness to 543 Ω/□ at 98 Å. The 98 Å sample was then annealed twice, first to 80 K, and then to 300 K. As a result its resistance at 10 K became 166 Ω/□ after the first annealing, and 100 Ω/□ after the second annealing. Films from set 2 (also on Si) are similar to set 1: we have observed  $R_\square = 20$  MΩ/□ at 26 Å and  $R_\square = 1000$  Ω/□ at 123 Å. Finally, films from

set 3, deposited on a Ge-coated glass substrate, range from 13 to 231 Å, while  $R_{\square}$  changes between 5.6 MΩ and 22.8 Ω.

The transmission coefficient of a film deposited on the substrate, measured relative to the transmission of the substrate itself, is related to real and imaginary parts of the sheet conductance of the film as [9]

$$T(\omega) = \frac{1}{[1 + Z_0\sigma'_{\square}(\omega)/(n + 1)]^2 + [Z_0\sigma''_{\square}(\omega)/(n + 1)]^2}. \quad (1)$$

Here  $Z_0 = 377 \Omega$  is the impedance of free space,  $n$  is the index of refraction of the substrate, equal to  $n_{Si} = 3.315$  for silicon and  $n_G = 1.44$  for glass, and  $\sigma'_{\square}(\omega)$  and  $\sigma''_{\square}(\omega)$  are, respectively, the real and imaginary parts of the sheet conductance of the film. Almost everywhere in our experiments  $\sigma'_{\square}(\omega), \sigma''_{\square}(\omega) \ll (n + 1)/Z_0$ . In this case the contribution of the imaginary part of conductance to the transmission coefficient is negligible and Eq. (1) can be approximately replaced by  $T(\omega) \approx [1 + Z_0\sigma'_{\square}(\omega)/(n + 1)]^{-2}$ . Throughout this Letter we use this approximation to extract the real part of the sheet conductance of the film from its transmission coefficient. Only for our thickest films we use the exact Eq. (1) to calculate parameters of the Drude fits as described below.

In Fig. 1 we plot the frequency-dependent conductance, extracted from the transmission data for the films from set 3 with the help of the above approximation to Eq. (1). The seven thickest films from this set exhibit a characteristic Drude falloff at high frequencies. For the rest of the films the conductivity systematically increases with frequency throughout our frequency range. The inset in Fig. 1 shows the inverse average ac conductance as well as the dc sheet resistance for set 3 as a function of thickness. Note that the curves start to deviate significantly from each other at around 50 Å.

In order to fit the conductance of our thickest films with the Drude formula, one needs to use the untruncated Eq. (1) for the transmission coefficient. Inserting the Drude expression for the sheet conductance  $\sigma_{\square}(\omega) = \sigma_D/(1 - i\omega\tau)$  directly into Eq. (1) one gets  $T(\omega)/[1 - T(\omega)] = (1 + \omega^2\tau^2)/[(\sigma_D/\sigma_0)^2 + 2\sigma_D/\sigma_0]$ , where  $\sigma_0 = (n + 1)/Z_0$ . Therefore, the transmission data, which are consistent with the Drude formula can be fitted with a straight line, when  $T(\omega)/[1 - T(\omega)]$  is plotted as a function of  $\omega^2$  (see Fig. 2). The knowledge of the average thickness of our films along with parameters  $\sigma_D$  and  $\tau$  of the Drude formula enables us to calculate the plasma frequencies in our films. They are shown in the inset in Fig. 2 as a function of  $1/\sigma_D$ —the dc sheet resistance in the Drude formula, which itself was extracted from our Drude fit. These results are in excellent agreement with the experimentally determined lead plasma frequency of  $\omega_p = 59\,400 \text{ cm}^{-1}$  [10]. In the remainder of this Letter we discuss possible

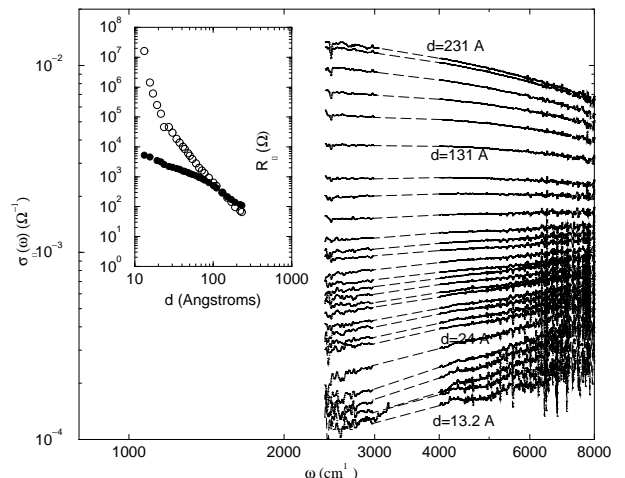


FIG. 1. Sheet conductance vs frequency for set 3. The dashed lines plotted between 3000 and 4000 cm<sup>-1</sup> (where the glass substrate is opaque) are a guide to the eye. The inset shows the inverse average ac conductance in our frequency range (solid circles) and the dc sheet resistance (open circles) as a function of the film thickness.

interpretations of the increase of the conductance with frequency, which we observe in our thinner films.

One mechanism which is known to cause a frequency dependence of the conductivity within a Drude plateau ( $\omega\tau \ll 1$ ) is purely quantum mechanical in origin. The conductivity is known to be reduced due to increased backscattering of phase-coherent electrons [so called weak localization (WL) [3]], as well as diffusion-enhanced electron-electron interactions (EEI) [4]. The magnitude of the WL reduction depends on the dephasing length  $L_\phi = \sqrt{D\tau_\phi}$  over which an electron maintains its phase coherence, while for EEI the correction depends on the

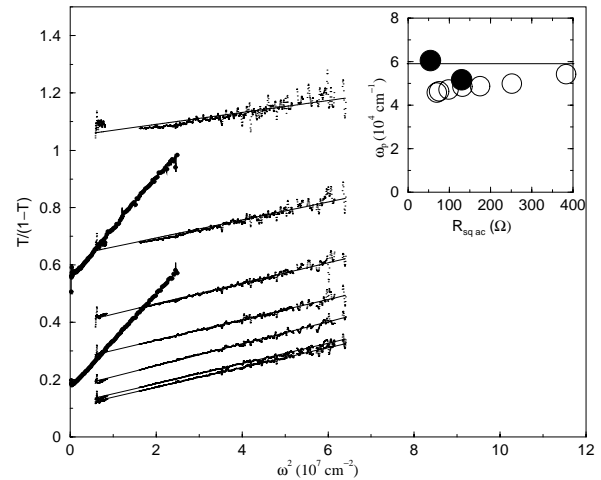


FIG. 2.  $T(\omega)/[1 - T(\omega)]$  vs  $\omega^2$  for the seven thickest films from set 3 (dots), and two annealed films from set 1 (solid circles). The solid lines are Drude model fits, as described in the text. The inset shows the plasma frequency extracted from these Drude fits with the solid line representing the plasma frequency of bulk lead from Ref. [10].

thermal coherence length  $L_T = \sqrt{\hbar D/kT}$ . For the ac conductivity the influence of the coherent backscattering is restricted to a spatial region of size  $L_\omega = \sqrt{D/\omega}$ . If this length scale turns out to be shorter than corresponding dc length scales, it is  $L_\omega$  which enters in all WL and EEI formulas. As in other cases, the effective dimensionality of a quasi-2D sample is decided by comparing the characteristic length scale ( $L_\omega$  in this case) to the film thickness  $d$ . The frequency-dependent WL corrections to the sheet conductance of the film are given by  $\Delta\sigma_{\square}^{2D}(\omega) = (e^2/2\pi^2\hbar)\ln\omega\tau$  in the 2D limit ( $d < L_\omega$ ) [3], and  $\Delta\sigma_{\square}^{3D}(\omega) = (\sqrt{2}e^2/4\pi^2\hbar)d\sqrt{\omega/D}$  in the 3D limit ( $d > L_\omega$ ) [5]. Using the lower end of our frequency range,  $\omega = 500 \text{ cm}^{-1}$ , and a realistic value of  $D = 5 \text{ cm}^2/\text{s}$  we can estimate that in our experiments  $L_\omega \leq 20 \text{ \AA} \leq d$ . Therefore, for our films one should use the formulas of three-dimensional localization theory. The frequency-dependent sheet conductance in most of our films is consistent with the  $\sqrt{\omega}$  dependence of 3D WL. However, we believe that in order to explain the frequency dependence of our experimental data one needs to look for yet another mechanism, supplementing that due to weak localization and electron-electron interactions. The problems with ascribing the observed frequency dependence of the conductivity solely to WL and EEI effects are (i) the dependence of the slope of the conductivity vs  $\sqrt{\omega}$  on the thickness of the film and the dc sheet conductance, which determines the diffusion coefficient  $D$ , does not agree with predictions of the 3D localization. (ii) The weak localization theory is supposed to work only in the limit where its corrections are much smaller than the dc conductivity. In our experimental data we do not see any change of behavior as the corrections to the conductivity become bigger than the dc conductivity. In fact the  $\sqrt{\omega}$  fit works very well and gives roughly the same slope even for films with a dc sheet resistance of  $\approx 100 \text{ k}\Omega$ , while the ac sheet resistance is only  $\approx 1 \text{ k}\Omega$ . Furthermore, the 3D-localization theory predicts that the  $\sqrt{\omega}$  dependence of weak localization theory crosses over to  $\omega^{(d-1)/d} = \omega^{1/3}$  dependence at or near the 3D metal-insulator transition [11]. In our experimental data we see no evidence for such a crossover.

There exists yet another, purely classical effect that gives rise to the frequency dependence of the conductivity. It is relevant in strongly inhomogeneous, granular films. There is ample experimental evidence that even ultrathin quenched-condensed films have a microscopic granular structure [12,13]. In order to describe the ac response of a film with such a granular microstructure one needs to know the geometry and conductivity of individual grains as well as the resistive and capacitive couplings between grains. The disorder, which is inevitably present in the placement of individual grains, makes this problem even more complicated. However, there exist two very successful approaches to the analytical treatment of such systems. One of them, known as the effective-medium

theory (EMT) [14] takes into account only concentrations of metallic grains and of the voids between the grains, disregarding any spatial correlations.

A more refined approach takes into account the geometrical properties of the mixture of metallic grains and voids. The insulator-to-metal transition in this approach is nothing else but the percolation transition, in which metallic grains first form a macroscopic connected path at a certain critical average thickness  $d_c$  of the film. The dc conductivity above the transition point scales as  $(d - d_c)^t$ , where  $t = 1.3$  in 2D and  $t = 1.9$  in 3D [6]. Just below the percolation transition the dielectric constant of the medium diverges as  $\epsilon(d) \sim (d_c - d)^{-s}$ , where  $s = 1.3$  in 2D and  $s = 0.7$  in 3D. The diverging dielectric constant is manifested as the imaginary part of the ac conductivity  $\sigma(\omega) \sim -i\omega(f_c - f)^{-s}$ . In general the complex ac conductivity of the metal-dielectric (void) mixture close to the percolation transition is known [6] to have the following scaling form:

$$\sigma(\omega, d) = |d - d_c|^t F_{\pm}(-i\omega|d - d_c|^{-(t+s)}). \quad (2)$$

Here  $F_+(x)$  and  $F_-(x)$  are scaling functions above and below the transition point, respectively. Note that this scaling form correctly reproduces the scaling of the dc conductivity above the transition and the divergence of the dielectric constant below the transition, provided that  $F_+(x) = F_+^{(0)} + F_+^{(1)}x + F_+^{(2)}x^2 + \dots$ , while  $F_-(x) = F_-^{(1)}x + F_-^{(2)}x^2 + \dots$ . One should mention that the predictions of the EMT can also be written in this scaling form with mean-field values of the exponents  $t = s = 1$ , and scaling functions  $F_{\pm}(x) = [\sqrt{D^2 + 4(D-1)x} \pm D]/[2(D-1)]$ , where  $D$  is the spatial dimension.

Since the metallic grains in our films form not more than two layers, our data should be interpreted in terms of the two-dimensional percolation theory. In two dimensions  $t = s = 1.3$  [6], and according to Eq. (2) the ac conductivity precisely at the transition point  $d = d_c$  is given by  $\sigma(\omega, d_c) = A(i\omega/\omega_0)^{t/(t+s)} = A(i\omega/\omega_0)^{1/2}$ . This prediction is in agreement with our experimental data. In Fig. 3 we attempt the rescaling of our data according to Eq. (2). The critical thickness  $d_c$  is determined as the point where the ac conductivity divided by  $\sqrt{\omega}$  is frequency independent. Of course, the experimental uncertainty in our data points does not allow us to determine which exponents  $t$  and  $s$  provide the best data collapse. However, as we can see from Fig. 3 our data are consistent with the scaling form of the 2D percolation theory. Finally, we use Fig. 3 to estimate basic parameters such as the typical resistance  $R$  of an individual grain and the typical capacitance  $C$  between nearest neighboring grains. From the limiting value of  $\sigma(\omega, d)(d_c/|d - d_c|)^{1.3}$  at small values of the scaling variable  $x = \omega(d_c/|d - d_c|)^{2.6}$  for  $d > d_c$ , one estimates the resistance of an individual grain to be of order of  $R \sim 1000 \Omega$ . In the simplest  $RC$  model, where

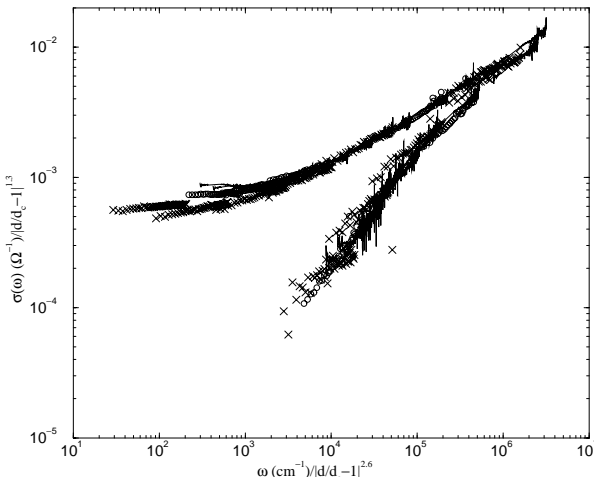


FIG. 3. The data collapse of the rescaled conductivity of 10 films from set 1 ( $d_c = 35.4 \text{ \AA}$ ,  $\times$ ), 9 films from set 2 ( $d_c = 48.4 \text{ \AA}$ , open circles), and 18 from set 3 ( $d_c = 34.2 \text{ \AA}$ , solid line).

a fraction of the bonds of the square lattice are occupied by resistors of resistance  $R$ , while the rest of the bonds are capacitors with capacitance  $C$ , the ac conductivity exactly at the percolation threshold is given by  $A/R(i\omega RC)^{1/2}$ , where  $A$  is a constant of order of one. Therefore, the slope  $\partial\sigma/\partial\sqrt{\omega}$  in our system should be of the same order of magnitude as  $\sqrt{RC}/R$ . This gives  $C \approx 2.6 \times 10^{-19} \text{ F}$ , which is in agreement with a very rough estimate of the capacitance between two islands  $200 \text{ \AA} \times 200 \text{ \AA} \times 30 \text{ \AA}$  separated by a vacuum gap of some  $20 \text{ \AA}$ , giving  $C \approx 2.7 \times 10^{-19} \text{ F}$ . This order of magnitude estimate confirms the importance of taking into account interisland capacitive coupling when one interprets the ac conductivity measured in our experiment. Indeed,  $R = 1000 \Omega$ , and  $C = 3 \times 10^{-19} \text{ F}$  define a characteristic frequency  $1/RC \approx 17000 \text{ cm}^{-1}$ , comparable to our frequency range.

In summary, we have measured the conductivity of ultrathin Pb films in the frequency range  $500\text{--}8000 \text{ cm}^{-1}$ . The evolution of  $\sigma(\omega)$  with dc sheet resistance is consistent with classical two-dimensional percolation theory in this range. At lower probing frequencies, where  $L_\omega$  becomes larger than the scale of inhomogeneities in these films, we expect that the effects of weak localization will become more prevalent.

We have benefited from fruitful discussions with P. B. Allen, A. M. Goldman, V. J. Emery, V. N. Muthukumar, Y. Imry, Z. Ovadyahu, and M. Pollak. The work at Brookhaven was supported by the U.S. Department of Energy, Division of Materials Sciences, under Contract No. DE-AC02-98CH10886. Support from NSF Grants No. DMR-9875980 (D.N.B.) and No. DMR-9725037

(B.N.) is acknowledged. Research undertaken at NSLS is supported by the U.S. DOE, Divisions of Materials and Chemical Sciences.

- [1] See, for example, M. Strongin, R. S. Thompson, O. F. Kammerer, and J. E. Crow, Phys. Rev. B **1**, 1078 (1970); E. G. Astrakharchik and A. I. Shalnikov, Sov. Phys. JETP **45**, 844 (1977); J. M. Graybeal and M. R. Beasley, Phys. Rev. B **29**, 4167 (1984); R. C. Dynes, A. E. White, J. M. Graybeal, and J. P. Gorno, Phys. Rev. Lett. **57**, 2195 (1986); N. Markovic, C. Christiansen, and A. M. Goldman, Phys. Rev. Lett. **81**, 5217 (1998); S.-Y. Hsu and J. M. Valles, Jr., Phys. Rev. Lett. **74**, 2331 (1995).
- [2] These phenomena were also actively studied in disordered layered oxide superconductors. See, for example, Y. Matsuda, S. Komiyama, T. Terashima, K. Shimura, and Y. Bando, Phys. Rev. Lett. **69**, 3228 (1992); M. Cieplak, S. Guha, S. Vadlamannati, T. Giebultowicz, and P. Lindenfeld, Phys. Rev. B **50**, 12876 (1994); J. Valles, A. E. White, K. T. Short, R. C. Dynes, J. P. Gorno, A. F. J. Levi, M. Anzlowar, and K. Baldwin, Phys. Rev. B **39**, 11599 (1989); S. I. Woods, A. S. Katz, M. C. deAndrade, J. Herrmann, M. B. Maple, and R. C. Dynes, Phys. Rev. B **58**, 8800 (1998).
- [3] For a review, see P. A. Lee and T. V. Ramakrishnan, Rev. Mod. Phys. **57**, 287 (1985).
- [4] For a complete discussion and many early references, see also B. L. Altshuler and A. G. Aronov, in *Electron-Electron Interaction in Disordered Systems*, edited by A. L. Efros and M. Pollak (North-Holland, Amsterdam, 1985).
- [5] L. P. Gorkov, A. I. Larkin, and D. E. Khmelnitskii, JETP Lett. **30**, 248 (1979).
- [6] An exhaustive review can be found at J. P. Clerc, G. Giraud, and J. M. Luck, Adv. Phys. **39**, 191 (1990).
- [7] D. B. Tanner, Y. H. Kim, and G. L. Carr, Mater. Res. Soc. Symp. Proc. **195**, 3 (1990); H. S. Choi, J. S. Ahn, J. H. Jung, T. W. Noh, and D. H. Kim, Phys. Rev. B **54**, 4621 (1996).
- [8] Y. Gefen, D. J. Thouless, and Y. Imry, Phys. Rev. B **28**, 6677 (1983).
- [9] M. Tinkham, *Introduction to Superconductivity* (McGraw-Hill, New York, 1975), p. 70; see also the original work of R. E. Glover III and M. Tinkham, Phys. Rev. Lett. **108**, 243 (1957).
- [10] M. A. Ordal *et al.*, Appl. Opt. **24**, 4493 (1985).
- [11] D. Vollhardt and P. Wölfle, Phys. Rev. Lett. **48**, 699 (1982).
- [12] K. L. Ekinci and J. M. Valles, Jr., Phys. Rev. B **58**, 7347 (1998); Phys. Rev. Lett. **82**, 1518 (1999).
- [13] K. Kagawa, K. Inagaki, and S. Tanda, Phys. Rev. B **53**, R2979 (1996).
- [14] D. A. G. Bruggeman, Ann. Phys. (Leipzig) **24**, 636 (1935).